

1 Concentration by pervaporation of representative
2 brown crab volatile compounds from dilute
3 model solution.

4 *Rodrigo Martínez, María Teresa Sanz*, Sagrario Beltrán*

5 Department of Chemical Engineering, University of Burgos, 09001 Burgos. Spain

6 In this work, the pervaporation technique is investigated in the separation of dilute
7 solutions of volatile compounds from brown crab effluent in order to obtain a valuable food
8 flavouring fraction. A systematic study of the pervaporation process has been carried out on
9 dilute model solutions of some of the compounds identified in the brown crab effluent as
10 typical volatile compounds. The membrane used in this work was a hydrophobic membrane
11 with a selective layer of POMS (polyoctylmethyl siloxane). The effect of some operating
12 variables, such as feed flow rate, feed concentration, feed temperature and permeate
13 pressure was analyzed on the pervaporation performance of the membrane.

14 *Keywords:* volatile compounds, concentration, pervaporation, POMS membrane

* Corresponding author. Tel.: +34 947 258810. Fax: +34 947 258831. E-mail address
tersanz@ubu.es

15 **1. Introduction**

16 Brown crabs are found in the Eastern Atlantic and are heavily exploited commercially
17 being available throughout the year. The brown crab liquid effluent produced during
18 boiling is believed to contain important amounts of volatile flavour components (Cha et al.
19 1993). This work is part of a wider study to consider the conversion of this by-product into
20 valuable volatile concentrate. Concentrates of the volatile species have considerable
21 commercial utility, especially in the food industry due to longer shelf life, reduced
22 packaging and lower distribution and storage costs (She and Hwang, 2006). Additionally,
23 organic removal from water at low concentrations involves an important environmental
24 challenge.

25 Cha et al. (1993) studied the concentration of the liquid effluent produced during snow crab
26 boiling by steam distillation. However, this technique involves high energy consumption as
27 well as physical aroma losses (García et al. 2008). In this work, the pervaporation process
28 has been considered to recover the volatile fraction from brown crab effluent.
29 Pervaporation is a membrane process which has been developed rapidly in the last 20 years
30 for aroma concentration (She and Hwang, 2006) since the addition of chemical solvents is
31 avoided. Additionally moderate operating temperatures help to minimize degradation of
32 aroma character.

33 Brown crab effluent was supplied by IDOKI SCF Technologies S.L. (Spain). The first step
34 in this work was to determine the main volatile organic compounds present in the industrial
35 effluent. More than 150 compounds were identified in the brown crab effluent. These
36 included mainly aldehydes, ketones, alcohols, esters, aromatic compounds and sulphur and
37 nitrogen-containing compounds. To study the ability of pervaporation process to recover

38 the volatile fraction from the brown crab effluent seven of the identified compounds have
39 been selected for a model aqueous solution of brown crab effluent: 1-octen-3-ol, 1-penten-
40 3-ol, 3-methylbutanal, hexanal, benzaldehyde, 2,3-pentadione and ethyl acetate.

41 A systematic study of the pervaporation process of the dilute model solution was performed
42 in order to analyze the influence of some operating variables on the pervaporation
43 performance. The permeation flux and enrichment factor of the selected volatile
44 compounds were analyzed at different operating conditions: feed flow rate, feed
45 temperature, feed concentration and permeate pressure.

46 **2. Theory.**

47 On the basis on the solution/diffusion model the flux of component i through the membrane
48 is proportional to the difference in partial vapor pressure at both sides of the membrane
49 (Blume et al. 1990):

$$50 \quad J_i = Q_{OV,i} (x_i \gamma_i p_i^s - y_i p_p) \quad (1)$$

51 where J_i is the partial permeation flux, $Q_{OV,i}$ the pressure-normalized permeation flux
52 (permeance), x_i the mole fraction of component i in the feed, γ_i the activity coefficient and
53 p_i^s the saturation vapor pressure at the temperature of the feed, y_i , the mole fraction in the
54 permeate and p_p the permeate pressure. In case of pervaporation of dilute aqueous solutions
55 activity coefficients at infinite dilution in water (γ_i^∞) are used as feed-side activity
56 coefficients due to the very low concentrations of aroma compounds in the feed (Trifunovic
57 and Trägårdh, 2006). In this work, the activity coefficients at infinite dilution in water were
58 estimated with the help of the software Aspen plus (2008) by using UNIQUAC equation

59 when binary interaction parameters were available, otherwise the predictive method
60 UNIFAC-Dortmund was used.

61 According to the resistance-in-series model, the two main mass transfer resistances that
62 affect the pervaporation process are the liquid boundary layer resistance and the membrane
63 resistance. At steady state the flux through the different mass transfer layers is equal:

$$64 \quad J_i = Q_{ov,i} (x_i \gamma_i p_i^s - y_i p_p) = k_{bl,i} \rho (x_i - x_i^m) = Q_{m,i} (p_i^m - y_i p_p) \quad (2)$$

65 where k_{bl} is the liquid boundary layer mass transfer coefficient, ρ the total mass volume
66 concentration of the feed, x_i^m mol fraction of i at the membrane-fluid interface, $Q_{m,i}$ the
67 pressure normalized permeation flux across the membrane and p_i^m the partial vapor
68 pressure of i at the membrane-fluid interface. The rest of the symbols are the same as in
69 Equation 1. The overall mass transfer coefficient in the steady state can be expressed as the
70 sum of these two resistances:

$$71 \quad \frac{1}{Q_{ov,i}} = \frac{\gamma_i p_i^s}{k_{bl,i} \rho} + \frac{1}{Q_{m,i}} \quad (3)$$

72 The term $\gamma_i p_i^s / \rho$ is the conversion factor from a concentration driving force to a partial
73 vapour pressure driving force. The overall mass transfer coefficient $Q_{OV,i}$ of Eq. 1 can be
74 obtained from experimental measurements of the permeate flux and feed concentration of
75 the permeating component i . The liquid boundary layer mass transfer coefficient, k_{bL} , is
76 related to the feed hydrodynamic conditions and it can be estimated from the Sherwood
77 correlation in terms of Reynolds (Re) and Schmidt (Sc) numbers for a plate-and-frame
78 module (Dotremont et al. 1994):

$$79 \quad Sh = \frac{k_{bl}d_h}{D_{i,water}} = 1.86 Re^{1/3} Sc^{1/3} \left(\frac{d_h}{L} \right)^{1/3} \quad (4)$$

80 where d_h is the hydraulic diameter, L a characteristic measure of the module defined by
 81 Dotremont et al. (1994) for a similar plate and frame module and $D_{i,water}$ the diffusion
 82 coefficient of i in water estimated using the Wilke-Chang correlation (Poling et al. 2001).

83 For pervaporation of dilute organic solutions, the boundary layer mass transfer resistance
 84 for water transport is assumed to be negligible (Ji et al. 1994):

$$85 \quad J_w = Q_w^m (p_w^s \gamma_w x_w - y_w p_p) \quad (5)$$

86 for dilute aqueous solutions activity coefficient and molar fraction of water are
 87 approximately equal to 1.

88 The separation performance of a pervaporation membrane can be described in terms of the
 89 permeation flux and the separation factor of the membrane (Huang and Rhim, 1991). The
 90 enrichment factor of a given component is the relationship between the concentration in the
 91 permeate and the feed:

$$92 \quad \beta_i = w_{i,p} / w_{i,f} \quad (6)$$

93 In dilute systems, as aroma recovery systems, the solvent enrichment factor is close to one,
 94 so aroma enrichment factors can be considered equal to the corresponding separation
 95 factors.

96 **3. Experimental section**

97 *3.1. Materials*

98 *Pervaporation membrane*

99 The membrane used in this work was a hydrophobic membrane kindly supplied by GKKS
100 Research Center (Germany). This membrane has a selective layer of POMS
101 (polyoctylmethyl siloxane) on a PEI (poly ether imide) support (batch 03/011).

102 Volatile compounds

103 The identification of the main volatile components present in the brown crab effluent was
104 performed by using a headspace-solid phase dynamic extraction-gas chromatography/mass
105 spectrometry (HS-SPDE-GC/MS). More than 150 compounds were identified in the brown
106 crab effluent. Among them, seven compounds have been selected for a model aqueous
107 solution of brown crab effluent. The selected volatile compounds belong to different
108 chemical classes: 1-octen-3-ol (Sigma Aldrich, 98 %), 1-penten-3-ol (Sigma Aldrich,
109 99 %), 3-methylbutanal (Sigma Aldrich, 97 %), hexanal (Sigma Aldrich, 98 %),
110 benzaldehyde (Sigma Aldrich, >=99 %), 2,3-pentadione (Sigma Aldrich, 98 %) and ethyl
111 acetate (Sigma Aldrich, HPLC grade). These compounds are characteristic of seafood
112 flavour: 1-octen-3-ol has been reported to be one of the volatile components widely
113 distributed in fresh and saltwater fish, 1-penten-3-ol contributes to a butter-like odor
114 (although its aroma treshold value is rather high), 3-methylbutanal is one of the most
115 abundant volatile compound in boiled and pasteurized crabmeat, hexanal is one of the most
116 abundant volatiles generated during lipid oxidation at moderate temperatures, benzaldehyde
117 contributes to characteristic cooked crab flavour and ketones such as 2,3 pentadione
118 contribute to the sweet floral, fruity flavour of many crustacean (Cha et al., 1993;
119 Josephson, 1990; Matiella and Hsieh, 1990). Ethyl acetate was also found in the brown
120 crab effluent and it was included in the model solution since could be considered as model
121 molecule (Baudot et al., 1999).

122 Table 1 summarizes the organoleptic characteristics of the selected volatile compounds
123 including the aroma threshold values (ATV), defined as the lowest concentration in a water
124 solution at which an aroma compound is perceptible. Table 2 lists some thermodynamic
125 properties of the selected compounds, including activity coefficients at infinite dilution and
126 vapor pressure of the volatile compounds. Vapor pressure correlations were obtained or
127 predicted by using Aspen Plus (2008) except for 2,3-pentadione which Antoine constants
128 were obtained from the literature (Soni et al., 2008). Figure 1 shows the vapor pressure of
129 the volatile compounds including water vapor pressure as a function of temperature.

130 *3.2. Feed solutions*

131 Different feed solutions were used in this work. First, pervaporation experiments were
132 performed using pure water as feed solution to check the performance of the POMS
133 membrane. Further, separations of binary mixtures (water/1-octen-3-ol) and
134 multicomponent mixtures were carried out in order to evaluate the influence of some
135 operating variables such as: feed flow rate, feed concentration, feed temperature and
136 permeate pressure on pervaporation performance.

137 *3.3. Pervaporation experiments*

138 The pervaporation experiments were performed under steady state with a plate and frame
139 laboratory stainless steel permeation cell (Sulzer Chemtech[®]) with an effective membrane
140 area in contact with the feed mixture of 170 cm² (Delgado et al., 2009). The temperature of
141 the feed liquid mixture was kept constant (± 0.5 °C) by using a thermostat to heat the stirred
142 tank feed reactor of 5 L capacity. Permeate pressure was regulated with an air-inlet located
143 between the condensers and the vacuum pump. The chemical stability of the membrane

144 was checked between each experiment, measuring pure water flux at reference operating
145 conditions.

146 *3.4. Sample analysis*

147 Permeate and feed concentrations were measured off-line using a Hewlett Packard (6890)
148 gas chromatograph (GC) equipped with series connected thermal conductivity (TCD) and
149 flame ionization (FID) detectors. Helium, 99.999 % pure, was used as carrier gas. The GC
150 column was a 007 FFAP 25 m × 0.25 mm bonded phase fused silica capillary column. The
151 injector and detectors were at 200 °C and 250°C respectively. The oven was operated at
152 programmed temperature, from 40°C to 220°C. 1-hexanol was used as internal standard for
153 analysis of the samples.

154 **4. Results and discussion**

155 *4.1 Pure water as feed solution*

156 The effect of feed temperature and permeate pressure on membrane performance was
157 studied using pure water as feed solution to check the behaviour of the POMS membrane.
158 Feed temperature was varied in the range 26 °C to 45 °C. By increasing feed temperature,
159 water permeation flux also increases mainly due to the increase of saturated water pressure
160 on the feed side of the membrane (Eq. 5). The temperature dependence of water permeation
161 flux, J_{water} , can be expressed by an Arrhenius-type relation:

$$162 \quad J_{\text{water}} = J_{\text{water},o} \exp\left(-E_{a,\text{water}}/RT\right) \quad (7)$$

163 where $E_{a,\text{water}}$ is the apparent activation energy of permeation, $J_{\text{water},o}$ the preexponential
164 factor and T the absolute temperature. An apparent activation energy of 46.65 kJ/mol

165 (Figure 2) was found by fitting water permeation flux obtained in this section (pure water
166 as feed solution) as well as water permeation flux obtained in the pervaporation of volatile
167 compounds dilute aqueous solutions (section 4.3).

168 Permeate pressure was varied in the range 100 Pa to 1200 Pa. Figure 3 shows the water
169 permeation flux dependence on permeate pressure. This Figure shows experimental data
170 obtained using pure water as feed solution and the results obtained in subsequent studies
171 (section 4.3). Figure 3 shows that by increasing the permeate pressure, water permeation
172 flux decreases as consequence of a decrease in the driving force (Equation 5). Water
173 permeances for the POMS membrane, calculated as the ratio of the permeation flux to the
174 permeant driving force, were constant whatever the feed temperature and permeate pressure
175 considered ($1.95 \cdot 10^{-7} \pm 1.23 \cdot 10^{-8} \text{ mols}^{-1} \text{ m}^{-2} \text{ Pa}^{-1}$ for all the experiments performed in this
176 work).

177 *4.2 Binary feed solution*

178 4.2.1 Boundary layer effect

179 First, the boundary layer effect was studied in the pervaporation of the binary system
180 water/1-octen-3-ol by varying the feed flow rate between 25 kg/h to 92 kg/h. According to
181 resistance-in-series model when boundary layer is dominant resistance, mass transfer
182 across the membrane increases with feed flow rate due to a decrease of the boundary layer
183 thickness. Figure 4 shows the effect of increasing feed flow rate on partial (water and 1-
184 octen-3-ol) permeation flux. Water and organic permeation fluxes were approximately
185 constant inferring that little concentration polarization takes place. The mass transfer
186 coefficient k_{bl} was calculated according to Sherwood correlation (Eq. 4). The relative
187 significance of the boundary layer mass transfer resistance was estimated less than 2% of

188 the total resistance in the range of feed flow rates studied in this work. However this result
189 must be carefully considered since Olsson and Tragardh (1999a) in their study of the
190 influence of feed flow velocity on pervaporative aroma recovery pointed out that Sherwood
191 correlation could overestimates the mass transfer coefficient of the liquid feed boundary
192 layer.

193 4.2.2. Effect of feed concentration

194 The effect of organic feed concentration was studied for water/1-octen-3-ol by varying the
195 volatile feed concentration in the range of 0.1 to 10 ppm. By increasing the concentration
196 of the volatile component in the feed solution, organic partial permeation flux increases. A
197 linear dependence of organic permeation flux can be assumed in the range of
198 concentrations studied in this work ($r^2 = 0.97$). However, water permeation flux remained
199 constant whatever the feed concentration (within the experimental error) and similar to the
200 values obtained when using pure water as feed solution. The mean value found for 1-octen-
201 3-ol enrichment factor was 37 ± 5 .

202 *4.3 Multicomponent feed solution*

203 Finally the effect of feed concentration, feed temperature and permeate pressure was study
204 in the pervaporation of a feed model solution consisting of seven volatile compounds: 1-
205 octen-3-ol, 1-penten-3-ol, 3-methylbutanal, hexanal, benzaldehyde, 2,3-pentadione and
206 ethyl acetate.

207 4.3.1. Effect of feed concentration

208 The feed concentration of all the organic compounds studied in this work was varied in the
209 range of 0.1 to 10 ppm at a fixed feed temperature (26°C) and permeate pressure (300 Pa).
210 Volatile organic concentration found in the brown crab effluent was rather low (less than 2

211 ppm). A wider range has been studied to minimize errors in the volatile organic compound
212 determination. Figure 5 shows an acceptable linear relationship between organic
213 permeation flux and feed concentration ($r^2 > 0.95$, except for benzaldehyde and 3-
214 methylbutanal, $r^2 = 0.93$). This behaviour indicates that a constant normalized permeation
215 flux (permeance) can be assumed in the studied concentration range. Figure 6 shows the
216 membrane permeance for the volatile compounds studied in this work as a function of
217 organic concentration in the feed. The greatest deviations were shown for benzaldehyde.
218 The lower values of the permeances correspond to 3-methylbutanal and ethylacetate, these
219 are the organic compounds with the greater vapour pressure. The enrichment factor for the
220 volatile compounds was independent of concentration in the range investigated in this
221 work. The observed tendency of enrichment factor was the following: $\beta_{1\text{-octen-3-ol}} (\approx 121) >$
222 $\beta_{\text{benzaldehyde}} (\approx 93) > \beta_{1\text{-penten-3-ol}} (\approx 25) > \beta_{\text{hexanal}} (\approx 22) > \beta_{2,3\text{-pentanedione}} (\approx 7) \approx \beta_{\text{ethylacetate}} (\approx 7) >$
223 $\beta_{3\text{-methylbutanal}} (\approx 5)$.

224 Water permeation flux remains constant and equal to the flux of pure water (within the
225 experimental error) whatever the feed concentration of the different aroma compounds.

226 Compared to the binary system previously studied 1-octen-3-ol shows an increase in
227 permeability in model multicomponent mixtures. This indicates that the presence of other
228 organic compounds in the feed solution can affect the membrane selectivity due to
229 interactions between the different aroma compounds. In this case a positive effect was
230 observed in the 1-octen-3-ol permeation. Other studies of the pervaporation of organic
231 compounds multicomponent mixtures (Isci et al., 2006; Kanani et al., 2003;
232 Sampranpiboon et al., 2000) have also observed positive or negative interactions between
233 the permeating aroma compounds. Isci et al. (2006) explained that higher fluxes than

234 expected can be obtained when a permeant of low diffusivity is dragged through the
235 membrane polymer by a permeant of higher diffusivity; the opposite can also happen.

236 4.3.2. Effect of feed temperature

237 Feed temperature is an important operating variable since it affects the feed/membrane
238 characteristics and the driving force of the process. The operating temperature was changed
239 in the range 26 °C to 35.7 °C at a fixed permeate pressure (300 Pa) and different fixed feed
240 concentration (0.1, 5 and 10 ppm). Moderate feed temperature is recommended in the study
241 of pervaporation of flavour compounds to avoid any damage to heat-sensitive compounds.
242 (She and Hwang, 2006). Figure 7 shows the effect of temperature on volatile compounds
243 permeation fluxes at an organic feed concentration of 10 ppm for all the volatile
244 compounds. For all the organic compounds, when the temperature increases the organic
245 permeation flux increases. The variation of the volatile compounds permeation flux with
246 temperature was found to follow an Arrhenius type relationship (Eq. 7). Apparent
247 activation energy for permeation of aroma compounds follows the order: $E_{a,\text{benzaldehyde}}$
248 (49.47 kJ/mol) < $E_{a,1\text{-octen-3-ol}}$ (58.64 kJ/mol) < $E_{a,\text{hexanal}}$ (79.55 kJ/mol) < $E_{a,1\text{-penten-3-ol}}$ (84.77
249 kJ/mol) < $E_{a,\text{ethylacetate}}$ (86.81) < $E_{a,3\text{-methylbutanal}}$ (87.66 kJ/mol) < $E_{a,2,3\text{pentadione}}$ (155.01 kJ/mol).
250 The apparent activation energy found for all volatile compounds is higher than that of water
251 ($E_{a,\text{water}} = 46.65$ kJ/mol). A higher value of the apparent activation energy indicates a more
252 sensitive behaviour towards temperature changes, inferring that water permeation flux is
253 less temperature dependence than that of volatile compounds. Therefore, the enrichment
254 factor of all volatile compounds increases with an increase in the feed temperature.
255 According to the values found for the apparent activation energy this trend was more
256 noticeable for the most volatile component than for the less volatile components considered

257 in this work. Figure 8 shows the enrichment factor at the three temperatures studied in this
258 work at a fixed feed concentration of 10 ppm for the volatile compounds. Similar behaviour
259 has been described in the literature in the recovery by pervaporation of different volatile
260 aroma compounds through different pervaporation membranes (Aroujalian and Raisi, 2007;
261 Olsson and Trägårdh, 1999b; Raisi et al., 2008). The results found in this section show a
262 strong dependence on temperature for 2,3-pentadione. Further studies are necessary to
263 confirm such behaviour.

264 With increasing temperature, the driving force increases because of the increasing vapour
265 pressure, and therefore the permeate flux will also increase (see Eq. 1). Additionally, an
266 increase in the operating temperature causes an increase in the motion of the polymer
267 chains improving the diffusion of the permeant molecules. Figure 9 shows the ratio of
268 partial permeation fluxes obtained at 35.7 °C and 26 °C for all the volatile compounds and
269 water. According to Olsson and Trägårdh (1999b) the contribution from improved diffusion
270 and increasing driving force to the increase of partial permeation flux has been also shown.
271 This Figure shows that for water and the less volatile components (benzaldehyde, 1-octen-
272 3-ol and 1-penten-3-ol) the increase in partial permeation flux is mainly due to an increase
273 in the driving force. However the contribution due to an increasing diffusion becomes
274 important for the more volatile compounds.

275 Enrichment factor values seem to decrease with the apparent activation energy values. The
276 activation energy that characterizes the temperature dependence of the membrane can be
277 estimated by subtracting the heat of vaporization (ranging from 35 kJ·mol⁻¹ for ethyl
278 acetate to 57 kJ·mol⁻¹ for 1-penten-3-ol) from the calculated apparent activation energy
279 (Feng and Huang, 1996). Activation energy of aroma compounds follows the order:
280 $E_{a,\text{benzaldehyde}} (-0.17 \text{ kJ/mol}) < E_{a,1\text{-octen-3-ol}} (8.26 \text{ kJ/mol}) < E_{a,1\text{-penten-3-ol}} (27.72 \text{ kJ/mol}) <$

281 $E_{a,\text{hexanal}}$ (36.73 kJ/mol) < $E_{a,3\text{-methylbutanal}}$ (50.23 kJ/mol) < $E_{a,\text{ethylacetate}}$ (51.57) < $E_{a,2,3\text{pentadione}}$
282 (116.82 kJ/mol). From the values of activation energy, it could be concluded that sorption
283 contributes more to permeation of 1-octen-3-ol and benzaldehyde molecules (the more
284 hydrophobic compounds and less volatile). In contrast, the permeation for the rest of the
285 volatile compounds studied in this work seems to be a diffusion dominating process.

286 4.3.3. Effect of permeate pressure

287 Permeate pressure is another operating parameter that affects the pervaporation
288 performance as well as the operating cost of the process (Raisi et al., 2008). Different
289 behavior was observed for organic permeation fluxes when varying permeate pressure in
290 the range studied in this work (100 Pa – 1800 Pa). Trifunovic et al. (2006) state that in
291 general components that are less volatile are more sensitive to changes in permeate
292 pressure than compounds with higher volatility due to their smaller driving force. Figure 10
293 presents the effect of permeate pressure on the enrichment factor of the aroma compounds
294 considered in this work. For the low volatile components (1-octen-3-ol and benzaldehyde)
295 the enrichment factor decreases as permeate pressure increases. However, other
296 components such as 1-penten-3-ol, hexanal and 2,3-pentadione are less sensitive to changes
297 in permeate pressure. Figure 10 shows that the enrichment factor of the components with
298 higher equilibrium vapour pressure than water (3-methylbutanal and ethyl acetate) tends to
299 increase as permeate pressure increases. These results agree with other findings that appear
300 on literature. According to Aroujalian and Raisi (2007) if the less volatile component is the
301 more rapidly permeating species, selectivity decreases as permeate pressure increases. On
302 the other hand, if the more rapidly permeating species are also the more volatile, selectivity
303 increases as permeate pressure increases. As pointed out by Wijmans et al. (1996), this

304 indicates a unique characteristic of pervaporation process since separation can be improved
305 by decreasing the driving force of the process.

306 **5. Conclusions**

307 In this work, the recovery of volatile components from a model solution was performed by
308 pervaporation with a POMS membrane. Pervaporation seems to be a promising technique
309 for the recovery of aroma compounds from brown crab effluent. POMS membrane has been
310 able to separate the organic compounds although organic partial permeation fluxes were not
311 very high. A constant water permeance was observed for all the experiments carried out in
312 this study. The membrane used in this work has shown higher selectivity towards the less
313 volatile components. Organic permeation fluxes increase with feed concentration as a
314 consequence of a higher driving force for the mass transport. In general partial permeation
315 fluxes and enrichment factors increase as the feed temperature increases. However different
316 behavior was observed for organic permeation fluxes with permeate pressure. As permeate
317 pressure increases enrichment factor of the less volatile component was found to decrease,
318 however for the most volatile components enrichment factors tend to increase by
319 decreasing the driving force of the process. Operating conditions can be optimized to obtain
320 permeates with a maximum organoleptic quality in its aroma profile. Further research is
321 needed to account the influence of other substances present in brown crab effluent such as
322 salt content.

323 **Nomenclature**

324 d_h = hydraulic diameter, m

- 325 $D =$ diffusion coefficient, $\text{m}^2 \cdot \text{s}^{-1}$
- 326 $E_a =$ apparent activation energy of permeation, $\text{kJ} \cdot \text{mol}^{-1}$
- 327 $J =$ mass permeation flux, $\text{g} \cdot \text{s}^{-1} \cdot \text{m}^{-2}$
- 328 $k_{bl} =$ liquid boundary layer mass transfer coefficient, $\text{m} \cdot \text{s}^{-1}$
- 329 $L =$ characteristics of the module, m
- 330 $p =$ pressure, Pa
- 331 $Q_{OV} =$ pressure-normalized permeation flux, $\text{g} \cdot \text{s}^{-1} \cdot \text{m}^{-2} \cdot \text{Pa}^{-1}$
- 332 $Q_m =$ pressure-normalized permeation flux across the membrane, $\text{g} \cdot \text{s}^{-1} \cdot \text{m}^{-2} \cdot \text{Pa}^{-1}$
- 333 $R =$ gas constant, $\text{kJ} \cdot \text{mol}^{-1} \text{K}^{-1}$
- 334 $T =$ absolute temperature, K
- 335 $x, y =$ mol fraction
- 336 $\rho =$ total mass volume concentration of the feed, $\text{g} \cdot \text{m}^{-3}$
- 337 $\gamma =$ activity coefficient
- 338 $\beta =$ enrichment factor
- 339 **upperscripts**
- 340 $i =$ component
- 341 $m =$ membrane
- 342 $p =$ permeate
- 343 $s =$ saturation

344 **Acknowledgments**

345 Financial support from the MICINN through CTQ2008-04999-PPQ is gratefully
346 acknowledged. R. Martinez acknowledges the JCyL Education Ministry.

347 **References**

348 Aroujalian, A., & Raisi A. (2007). Recovery of volatile aroma components from orange
349 juice by pervaporation. *J. Membr. Sci.*, 303, 154-161.

350 Aspen Plus V7.1 (2008) Aspen Technology, Inc., 2008.

351 Baudot, A., Souchon, I., & Marin, M. (1999). Total permeate pressure influence on the
352 selectivity of the pervaporation of aroma compounds. *J. Membr. Sci.*, 158, 167-185.

353 Blume, I., Wijmans, J.G., & Baker, R. W. (1990). The separation of dissolved organics
354 from water by pervaporation. *J. Membr. Sci.*, 49, 253-286.

355 Cha, Y.J., Cadwallader, K.R., & Baek, H.H. (1993). Volatile flavor components in snow
356 crab cooker effluent and effluent concentrate. *J. Food Sci.*, 58, 525-530.

357 Delgado, P., Sanz, M.T., & Beltrán, S. (2009). Pervaporation of the quaternary mixture
358 present during the esterification of lactic acid with ethanol. *J. Membr. Sci.*, 332, 113-120.

359 Dotremont, C., Van den Ende, S., Vandommele, H., & Vandecasteele, C. (1994).
360 Concentration polarization and other boundary layer effects in the pervaporation of
361 chlorinated hydrocarbons. *Desalination*, 95, 91-113.

362 Feng, X.; & Huang, R.Y.M. (1996). Estimation of activation energy for permeation in
363 pervaporation processes. *J. Membr. Sci.*, 118, 127-131.

364 Flavor-Base Professional (2007), Lefingwell & Associates.

365 García, V., Diban, N., Gorri, D., Keiski, R., Urtiaga, A., & Ortiz, I. (2008). Separation and
366 concentration of bilberry impact aroma compound from dilute model solution by
367 pervaporation. *J. Chem. Technol. Biotechnol.*, 83, 973-982.

368 Huang, R.Y.M., & Rhim, J.W. (1991) Separation characteristics of pervaporation membrane
369 separation processes. In Elsevier (Ed.), *Pervaporation Membrane Separation Processes*
370 (pp. 111-180). Amsterdam.

371 Isci, A., Sahin, S., & Sumnu, G. (2006). Recovery of strawberry aroma compounds by
372 pervaporation. *J. Food Eng.*, 75, 36-42.

373 Ji, W., Hilalyb, A., Sikdarb, S.K., & Hwang, S.T. (1994). Optimization of multicomponent
374 pervaporation for removal of volatile organic compounds from water. *J. Membr. Sci.*, 97,
375 109-125.

376 Josephson, D.B. (1991). Seafood. In Marcel Dekker (Ed.), *Volatile compounds in Foods*
377 *and Beverages* (pp. 179-202). New York.

378 Kanani, D.M., Nikhade, B.P., Balakrishnan, P., Singh, G., & Pangarkar, W.G. (2003).
379 Recovery of valuable tea aroma components by pervaporation. *Ind. Eng. Chem. Res.*, 42,
380 6924-6932.

381 Matiella, J., & Hsieh, T.C. (1990). Analysis of crabmeat volatile compounds. *J. Food Sci.*,
382 55, 962-966.

383 Olsson, J., & Tragardh, G. (1999a). Influence of feed flow velocity on pervaporative aroma
384 recovery from a model solution of apple juice aroma compounds. *J. Food Eng.*, 39, 107-
385 115.

386 Olsson, J., & Tragardh, G. (1999b). Influence of temperature on membrane permeability
387 during pervaporative aroma recovery. *Sep. Sci. Technol.*, 34, 1643-1659.

388 Poling, B.E., Prausnitz, J.M., & O'Connell, J.P. (2001). Diffusion Coefficients. In
389 McGraw-Hill (Ed.), *The Properties of Gases and Liquids* (pp. 11.1-11.55). New York.

390 Raisi, A., Aroujalina, A., & Kaghazchi, T. (2008). Multicomponent pervaporation process
391 for volatile aroma compounds recovery from pomegranate juice. *J. Membr. Sci.*, 322, 339-
392 348.

393 Sampranpiboon, P., Jiraratananon, R., Uttapap, D., Feng, X., & Huang, R.Y.M. (2000).
394 Separation of aroma compounds from aqueous solution by pervaporation using
395 polyoctylmethylsiloxane (POMS) and polydimethylsiloxane (PDMS) membranes. *J.*
396 *Membr. Sci.*, 174, 55-65.

397 She, M., & Hwang, S.-T. (2006). Recovery of key components from real flavour
398 concentrates by pervaporation. *J. Membr. Sci.*, 279, 86-93.

399 Soni, M., Ramjugernath, D., & Raal, J.D. (2008). Vapor-Liquid Equilibrium for binary
400 systems of 2,3-pentanedione with diacetyl and acetone. *J. Chem. Eng. Data*, 53, 745-749.

401 Trifunovic, O., & Trägårdh, G. (2006). Mass transport of aliphatic alcohols and esters
402 through hydrophobic pervaporation membranes. *Sep. Purif. Technol.*, 50, 51-61.

403 Trifunovic, O., Lipnizki, F., & Trägårdh, G. (2006). The influence of process parameters on
404 aroma recovery by hydrophobic pervaporation. *Desalination*, 189, 1-12.

405 Wijmans, J.G., Athayde, A.L., Daniëls, R., Ly, J.H., Kamaruddin, H.D., & Pinnau, I.
406 (1996). The role of boundary layers in the removal of volatile organic compounds from
407 water by pervaporation. *J. Membr. Sci.*, 109, 135-146.

408

409 **Table 1.** Aroma compounds used in the model solution (Flavor-Base Professional, 2007).

Aroma compound	Organoleptic characteristics	ATV, ppb
1-Octen-3-ol	Very strong, sweet, earthy mushroom odor and taste	1.0
1-Penten-3-ol	Pungent, grassy, alliaceous-like, green vegetable, fruity taste	400
3-Methylbutanal	Powerful, penetrating, cheesy-sweaty-fruity in dilution	0.2-2
Hexanal	Strong, penetrating, fatty-green, grassy unripe fruit odor	4.5
Benzaldehyde	Odor of bitter almond oil, characteristic sweet cherry taste	350
2,3-Pentadione	Oily-buttery, fatty odor, butter, cream, milk taste	30
Ethyl Acetate	Ethereal, sharp, wine-brandy like odor	5.0

410

411

412

413 **Table 2.** Physicochemical properties of the volatile compounds

Compound	1-Octen-3-ol	1-Penten-3-ol	3-Methylbutanal	Hexanal	Benzaldehyde	2,3-Pentadione	Ethyl acetate
MW	128.2	86.1	86.1	100.2	106.1	100.1	88.1
BP (°C)	174-5	114.4	92.5	128.3	178.8	108	77.1
p^s (26°C), Pa	65	1348	7035	1540	181	2918	13045
γ^{∞} (26°C)	4955.4	17.0	164.6	1047.2	273.7	282.4	75.3
VM ^{BP} (cc/mol)	186.6	117	118.9	140.0	118.6	121	106.3

414

415 **List of Figure Caption**

416 **Figure 1.** Vapor pressure of water and volatile compounds as a function of temperature.

417 **Figure 2.** Effect of temperature on water permeation flux ($p_p = 300$ Pa).

418 **Figure 3.**Effect of permeate pressure on water permeation flux ($T = 26^\circ\text{C}$).

419 **Figure 4.** Water (\blacktriangle) and 1-octen-3-ol (i, Δ) permeation flux at different Reynolds ($p_p =$
420 400 Pa, $T = 26^\circ\text{C}$, $C_{i,\text{feed}} \approx 5$ ppm).

421 **Figure 5.** Effect of volatile feed concentration on volatile compound permeation flux ($T =$
422 26°C , $p_p = 300$ Pa).

423 **Figure 6.** Volatile compound permeance as a function of volatile feed concentration ($T =$
424 26°C , $p_p = 300$ Pa).

425 **Figure 7.** Effect of feed temperature on volatile compound permeation flux ($C_{i,\text{feed}} \approx$
426 10 ppm, $p_p = 300$ Pa).

427 **Figure 8.** Enrichment factor of volatile compound at different operating temperatures
428 ($C_{i,\text{feed}} \approx 10$ ppm, $p_p = 300$ Pa).

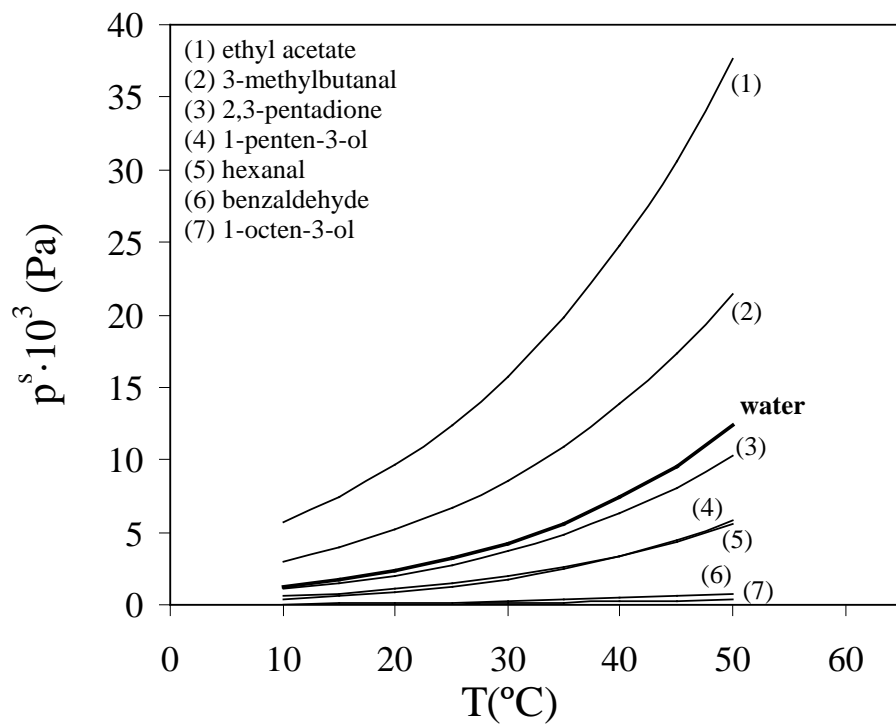
429 **Figure 9.** Ratio of volatile compound permeation flux at 35.7°C and 26°C .

430 **Figure 10.** Enrichment factor of volatile compound at different operating permeate
431 pressure ($C_{i,\text{feed}} \approx 10$ ppm, $T = 26^\circ\text{C}$).

432

433

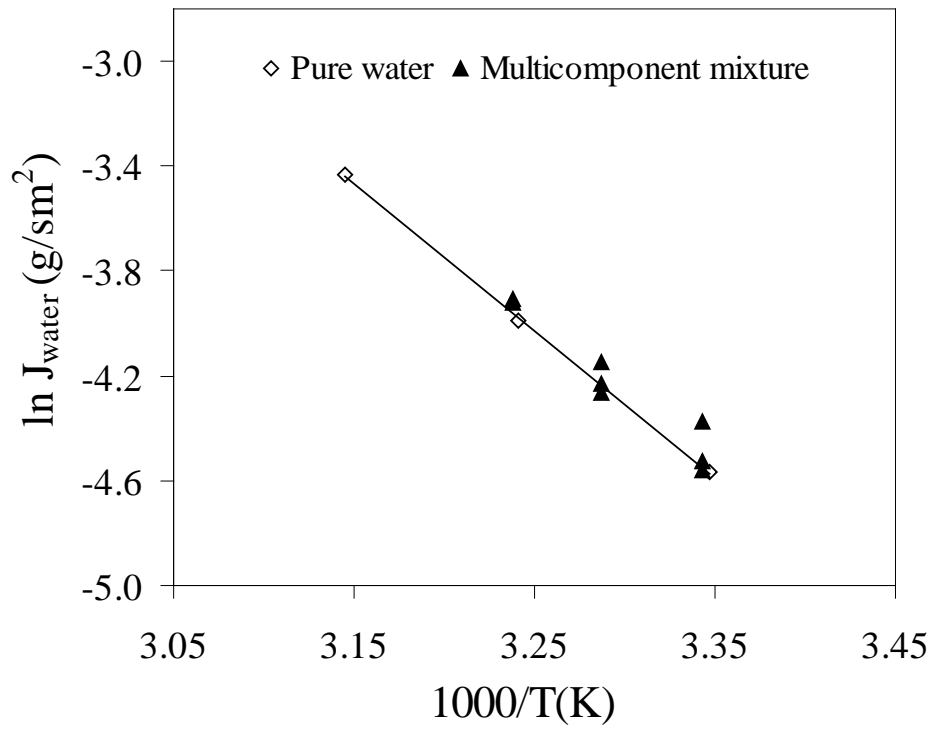
434
435
436
437
438
439
440



441
442
443
444
445
446

Figure 1. Vapor pressure of water and volatile compounds as a function of temperature.

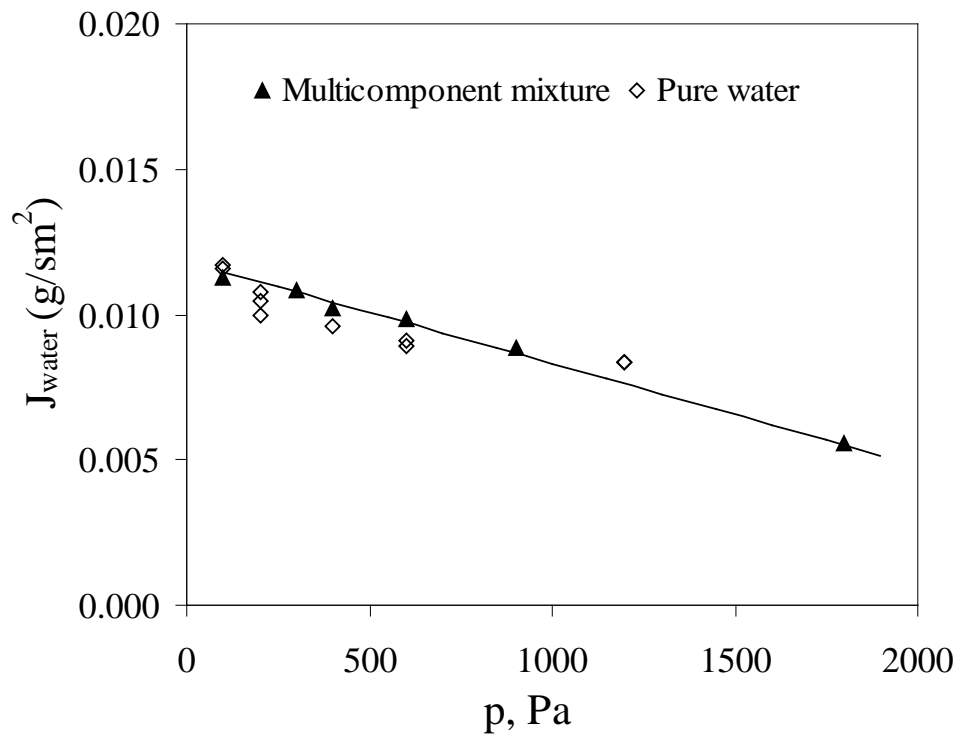
447
448
449
450
451
452



453
454
455
456

Figure 2. Effect of temperature on water permeation flux ($p_p = 300 \text{ Pa}$).

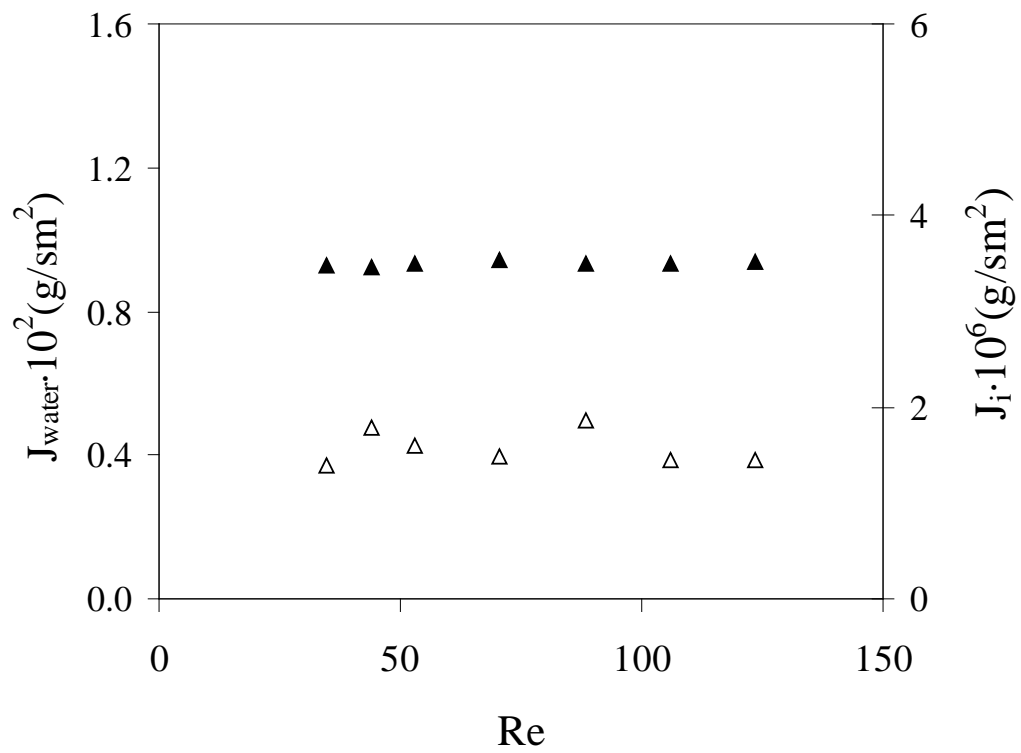
457
458
459
460
461
462



463
464
465
466

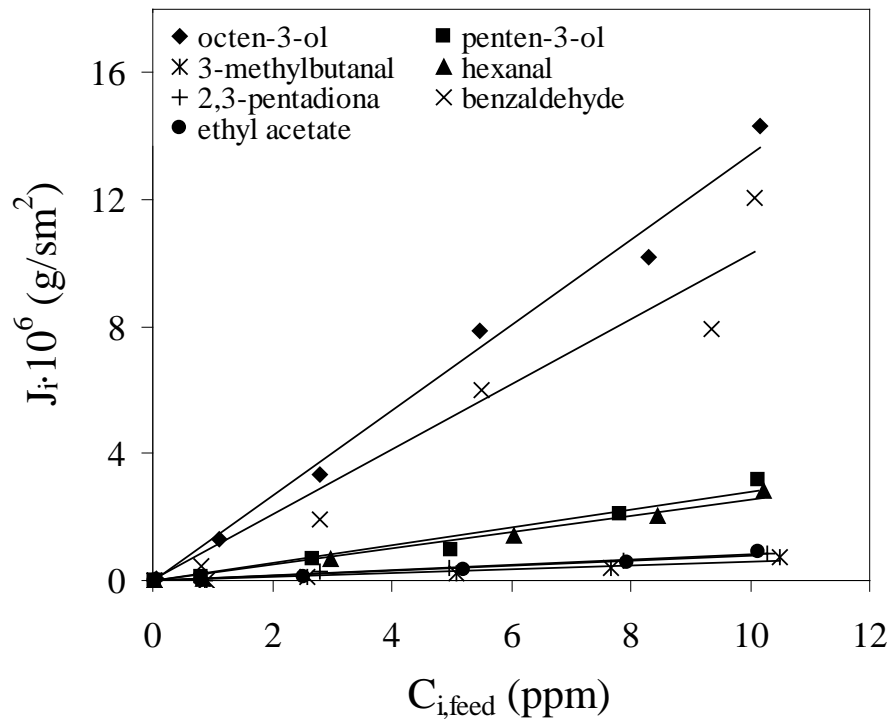
Figure 3. Effect of permeate pressure on water permeation flux (T = 26°C).

467
468
469
470
471
472



473
474 **Figure 4.** Water (▲) and 1-octen-3-ol (i, Δ) permeation flux at different Reynolds ($p_p =$
475 400 Pa, $T = 26^\circ\text{C}$, $C_{i,\text{feed}} \approx 5 \text{ ppm}$).
476

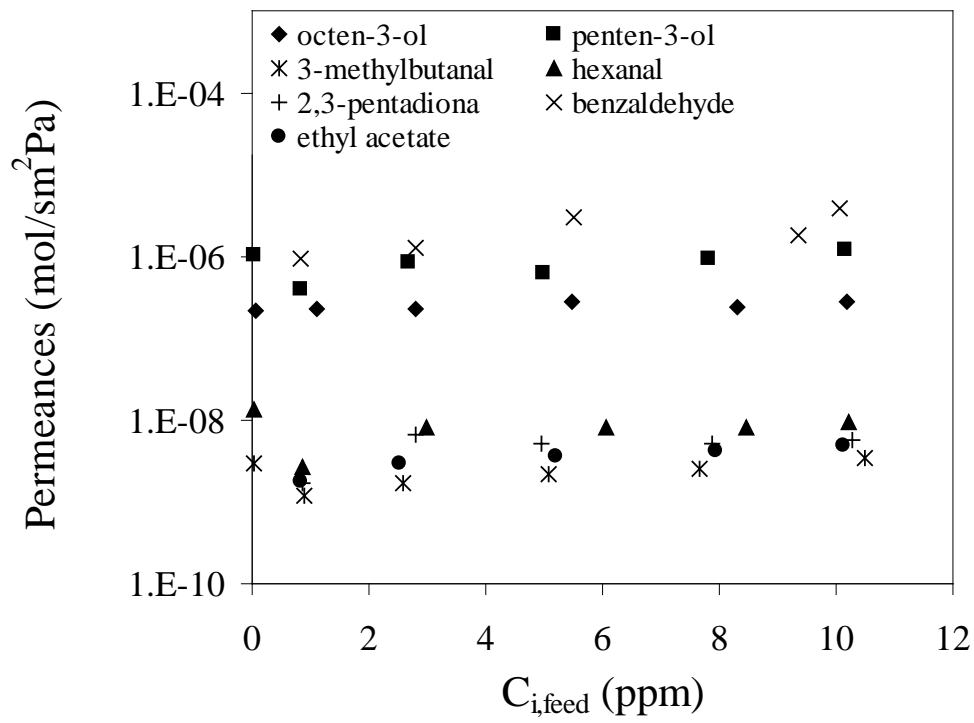
477
478
479
480
481
482



483
484
485
486
487

Figure 5. Effect of volatile feed concentration on volatile compound permeation flux ($T = 26\text{ }^\circ\text{C}$, $p_p = 300\text{ Pa}$).

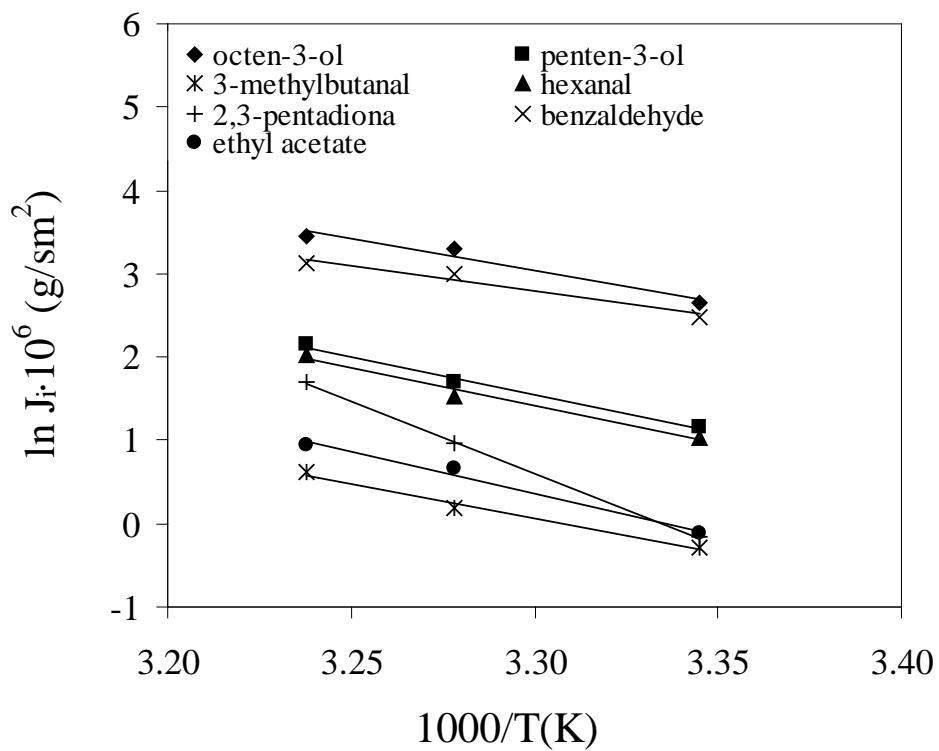
488
489
490
491
492
493



494
495
496
497
498

Figure 6. Volatile compound permeance as a function of volatile feed concentration (T = 26 °C, p_p = 300 Pa).

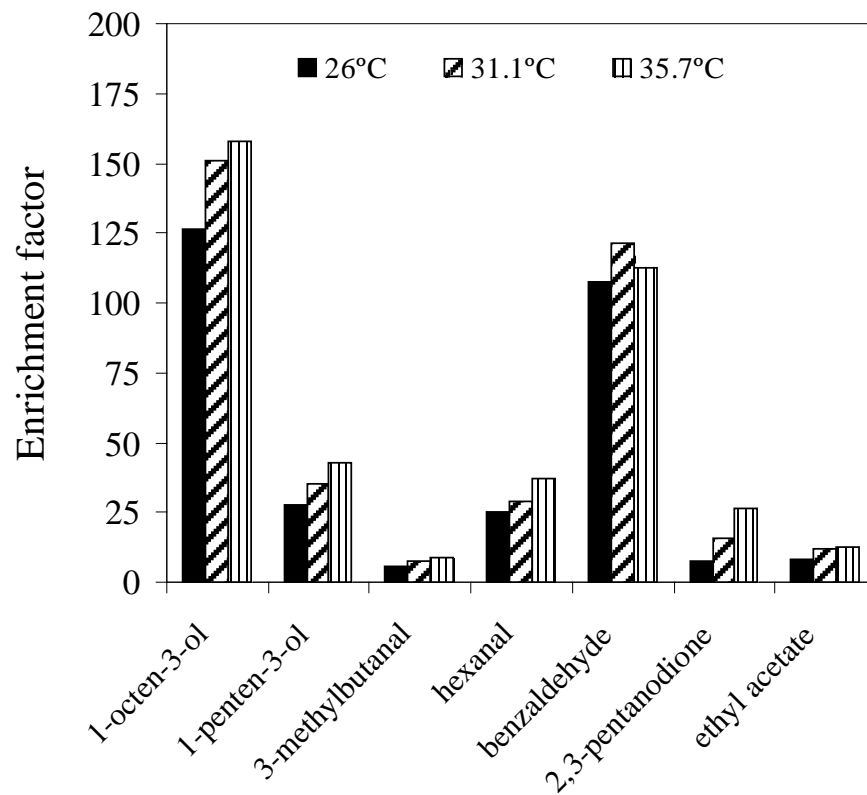
499
500
501
502
503
504



505
506
507
508
509

Figure 7. Effect of feed temperature on volatile compound permeation flux ($C_{i, \text{feed}} \approx 10$ ppm, $p_p = 300$ Pa).

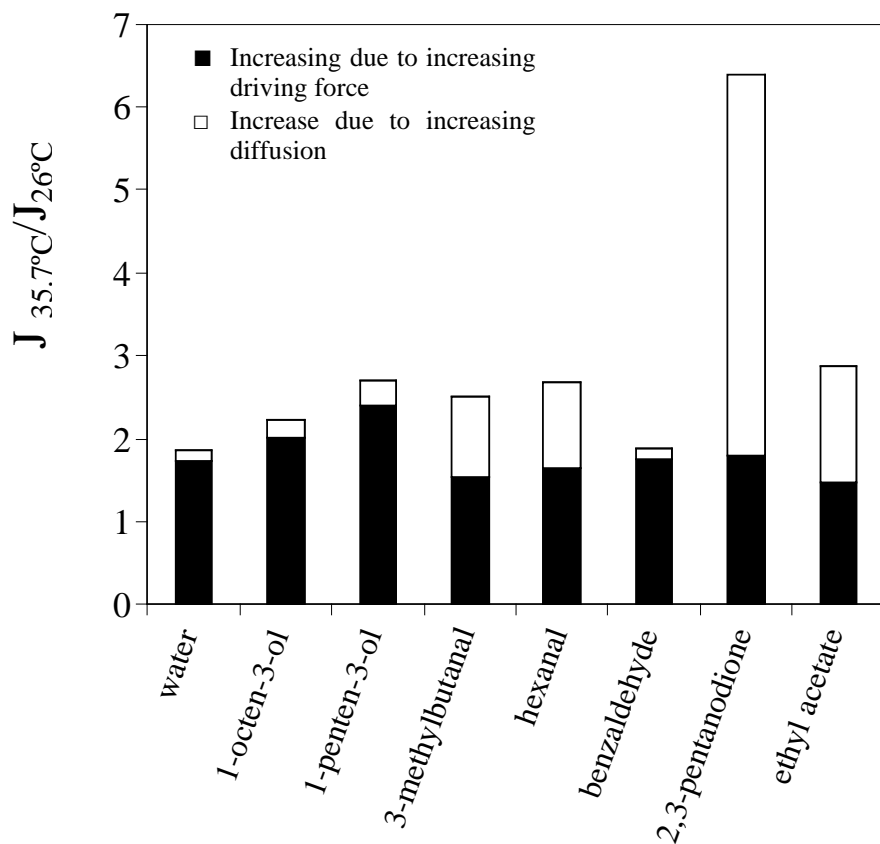
510
511
512
513
514
515



516
517
518
519
520
521

Figure 8. Enrichment factor of volatile compound at different operating temperatures ($C_{i,feed} \approx 10$ ppm, $p_p = 300$ Pa).

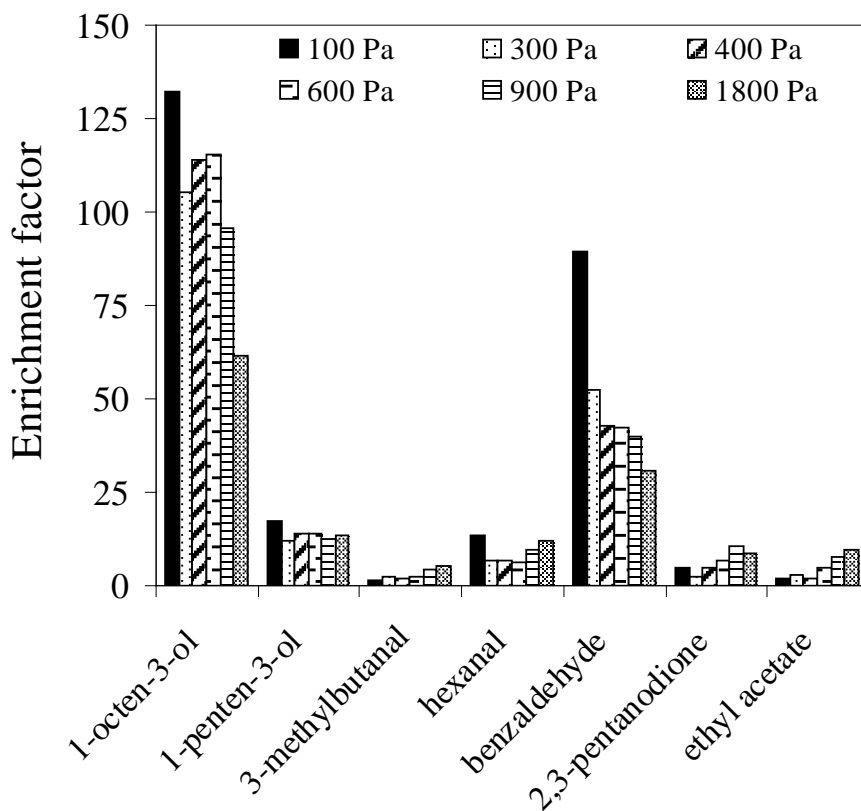
522
523
524
525
526
527
528



529
530
531

Figure 9. Ratio of volatile compound permeation flux at 35.7 °C and 26°C.

532
533
534
535
536
537



538
539
540
541
542

Figure 10. Enrichment factor of volatile compound at different operating permeate pressure ($C_{i,feed} \approx 10$ ppm, $T = 26$ °C).